The cochlea depicted: radiological evaluation of cochlear morphology and the implanted cochlea

Jagt, M.A. van der

Chapter 5

Improved cochlear implant position detection with spatially synchronized pre- and post-operative midmodiolar cross-section CT and MR images

MA van der Jagt, JJ Briaire,
S Boehringer, BM Verbist, JHM Frijns

Under review

Abstract

Objectives: In vivo evaluation of intrascalar position of a cochlear implant electrode array provides surgical feedback but is challenging due to scattering effects of the electrode array. This study introduces and assesses an evaluation method using spatially synchronized pre- and post-operative midmodiolar cross-sections of CT and MR images.

Methods: Three observers scored the intra-scalar position of all electrode contacts of 15 HiFocus 1J and 15 HiFocus Mid-Scala electrode arrays using 3 different methods; on midmodiolor cross-sections in post-operative CT images only (1), supported with spatially synchronized pre-operative CT (2) or MR (3) images. The intra- and inter-observer coefficients were calculated and compared between the 3 methods.

Results: Using spatially synchronized pre-operative images increases inter-observer coefficients in the 1J population from 0.75 to 0.79 and 0.80 with the use of pre-operative CT and MRI, respectively. In the MS population an increase from 0.77 to 0.83 (CT and MR) was found. For the intra-observer correlation coefficients, increases from 0.72 to 0.81 (CT) and 0.82 (MR) in the 1J and from 0.72 to 0.86 (CT) and 0.84 (MR) in the MS population were seen. No difference between the use of CT and MR images was found. A significant effect of angular insertion depth on the inter- and intra-observer coefficients was found in the MS population only, with increased coefficients for the more apical electrode contacts. Additionally, the use of a pre-operative framework increased the degree of certainty in allocations.

Conclusion: Using a referential pre-operative CT or MR scan improves the detection of scalar position and translocation of cochlear implants electrode array position.

Introduction

Cochlear implantation carries the risk of damaging intra-cochlear structures when inserting the electrode array into the cochlea. This damage may result in degeneration of neural structures, which could inhibit electrical stimulus transmission to the auditory cortex. Translocation of the array from the scala tympani to vestibuli will also lead to an increased distance between a contact and the spiral ganglion cells, hereby further adding to suboptimal stimulation. Although not conclusively proven, it is postulated that preservation of the intra-cochlear architecture is crucial for optimal hearing outcomes and that intra-cochlear damage might contribute, at least in part, to inter-patient variability in word recognition and residual hearing.1 Moreover, for long-term purposes, preventing trauma facilitates the re-implantation of new devices. Therefore, detection and limitation of insertion trauma plays a crucial role in optimizing both short- and long-term performance, following cochlear implantation.

Evaluation of cochlear implant position additionally provides feedback on surgical procedures and implant designs and it can support fitting procedures. By in vivo assessment of the CI electrode array position, correlations between the precise position and clinical outcome can be examined in a large cohort of patients. To evaluate their position, structures that indicate the partitioning of the cochlear duct, like the osseous interscalar septum and soft structured basilar and Reissner's membranes, play an important role. Micro-CT depicts fine intra-cochlear structures in high detail, due to the high spatial resolution and also histological examination provides accurate details on both osseous and soft tissue structures. However, both histological and micro-CT analyses are only applicable in cadaveric studies, which are typically carried out in small series.

In a clinical setting high resolution CT scans or Cone beam CT scans can be used for post-implantation evaluations. However, the accuracy of clinical CT scans for evaluation of cochlear trauma may be degraded by the metal blooming artefacts caused by the electrode array. This blooming effect obscures the scalar bounderies, which are crucial to determine the electrode array position. The use of midmodiolar cross-sectional CT images for the determination of cochlear implant electrode array positions was validated with anatomic microdissections, in a study by Lecerf et al.[2] To be more specific about the intra-scalar position, a linear 5-point grading scale was introduced by Helbig et al.[3] and Connor et al.[4] This approach offered a simple, but standardized method. Yet, the authors report that it became increasing difficult to correctly determine the position of the electrode carrier beyond 360 degrees.

The aim of this present study was to evaluate and compare the clinical reliability of three methods for determining the position of a cochlear implant electrode array on post-operative

CT images, based on the principle of combining pre- and postoperative midmodiolar cross-sectional images. The following three methods were carried out; evaluation on midmodiolor cross-section post-operative CT images only (1), supported with spatially synchronized pre-operative CT (2) or MR (3) images.

Materials & Methods

Patient population and implant designs

To test the method in patients with both translocated and non-translocated electrode arrays, we conducted a prior screening assessment of post-operative CT scans from patients that received cochlear implants between 2012 and 2015. We selected 30 adult patients with normal inner ear anatomy, that underwent unilateral implantation of a pre-curved HiFocus Mid-Scala (MS; n=15) or a straight HiFocus 1J (1J; n=15) electrode array (Advanced Bionics, Valencia, CA). The MS electrode is a pre-curved array, designed to achieve a mid-scalar position. It contains 16 electrode contacts and total active length of the array from basal contact to the tip is 15 mm. The distance from tip to the proximal blue marker that indicates a full insertion is 18 mm. The cross-sectional diameter varies from approximately 0.5 mm at the most apical contact to approximately 0.7 mm at the most basal contact. The 1J electrode array is a less pre-curved array, designed for outer wall positioning. It also contains 16 electrode contacts, leading to a total length of the array from basal contact to the tip of 17 mm. There is an additional 3 mm length from the most basal contact to the marker contact, indicating that a full insertion is 20 mm. The cross-sectional diameter of the array varies from approximately 0.4 mm at the most apical contact to approximately 0.8 mm at the most basal contact. Patient demographics are described in Table 1.

Radiological evaluation

All 30 patients received 3T MRI (Philips Achieva or Ingenia; Philips Healthcare, Best, The Netherlands) and multi-slice CT (MSCT; Aquilion; Toshiba Medical Systems, Otoware, Japan) examinations prior to implantation. An MSCT examination was also performed 1 day post-implantation, according to the standard work-up for patients with cochlear implants at our medical institution. Subsequently, multiplanar reconstructions were created from all 3 scans. The multiplanar reconstructions were based on a plane that ran through the basal cochlear turn, which provided the commonly used cochlear view, and a perpendicular line that ran through the modiolar axis. Within these reconstructions, the 3-dimensional (3D) consensus coordinate system was applied, as described by Verbist et al. [5] This framework included three consistent landmarks: the cochlear apex, the round window, and the most lateral part of the lateral semicircular canal. Thus, measurements could be directly compared between any original 3D datasets that included these landmarks; i.e., preoperative CT and MRI inner ear datasets. With this coordinate system, the location of the round window was defined

in the pre-operative CT image and applied to both the pre-operative MRI and the post-operative CT images. Subsequently, the centre of each electrode contact was determined manually.[6] A custom algorithm was written using MATLAB and its image processing toolbox (version R2015a) to present the spatially synchronized midmodiolar images adjacently, based on the coordinates of each electrode contact that determined the angle of cross-section in both MPRs.

Evaluation of intra-scalar electrode contact positions

Three methods were compared to evaluate the individual positions of 16 electrode contacts (Figure 1). The first method required a single midmodiolar cross-sectional image of the post-operative CT (Figure 1A). In this method, the scalar position of the electrode contact was determined based solely on the information provided in the post-operative scan. The second method combined the pre-operative (Figure B) and post-operative (Figure A2) CT scans, acquired at the exact same angular position from the round window and presented side by side. Thus, the pre-operative scan served as a referential framework by depicting the osseous spiral lamina and interscalar septum, which are commonly less visible on the post-operative CT scan, due to the presence of the array and the blooming artefacts caused by its metallic components. However, Figure 1B shows that the cochlear boundaries beyond the first turn were more poorly depicted, because the smaller structures become less resolved with progression from the basal to apical ends. This may impede accurate determination of the position of the more apical electrode contacts. In an attempt to overcome this limitation, a third method was conceived. In this method, the pre-operative 3T MRI (C) was acquired at the same angular position from the round window as the post-operative CT scan (A3). When these images were presented adjacent to one another, they provided additional, more distinct information on the second and third cochlear turns.

Three observers with different levels of experience judged each individual electrode contact twice for each evaluation method. Observer A is an experienced radiologist specialized in head and neck radiology, observer B is an ENT-surgeon in training and PhD student with training and sustained practice in imaging of the temporal bone, observer C is a PhD student focussing on speech coding strategies in cochlear implantation, without experience in imaging of the temporal bone. Observer 3 was instructed to evaluate midmodiolar cross-sections of cochlear images by observer 2. A score between 0 and 5 was assigned that reflected the position of the electrode contact within the cochlear lumen.[3,4] Scores 1 and 2 indicated a ST position; scores 4 and 5 indicated a SV position, with different degrees of certainty. Thus, a score of 1 reflected a certain and 2 reflected a likely ST position; a score of 5 reflected a certain and 4 reflected a likely SV position. A score of 3 could be chosen for an intermediate position, and a score of 0 was given when the observer was unable to assess the position. The observers could adjust the Houndsfield settings and use the zoom

tool to optimize evaluations of the cross-sectional images. The scans were presented in randomized order, and the observers were blinded to patient name and electrode design.

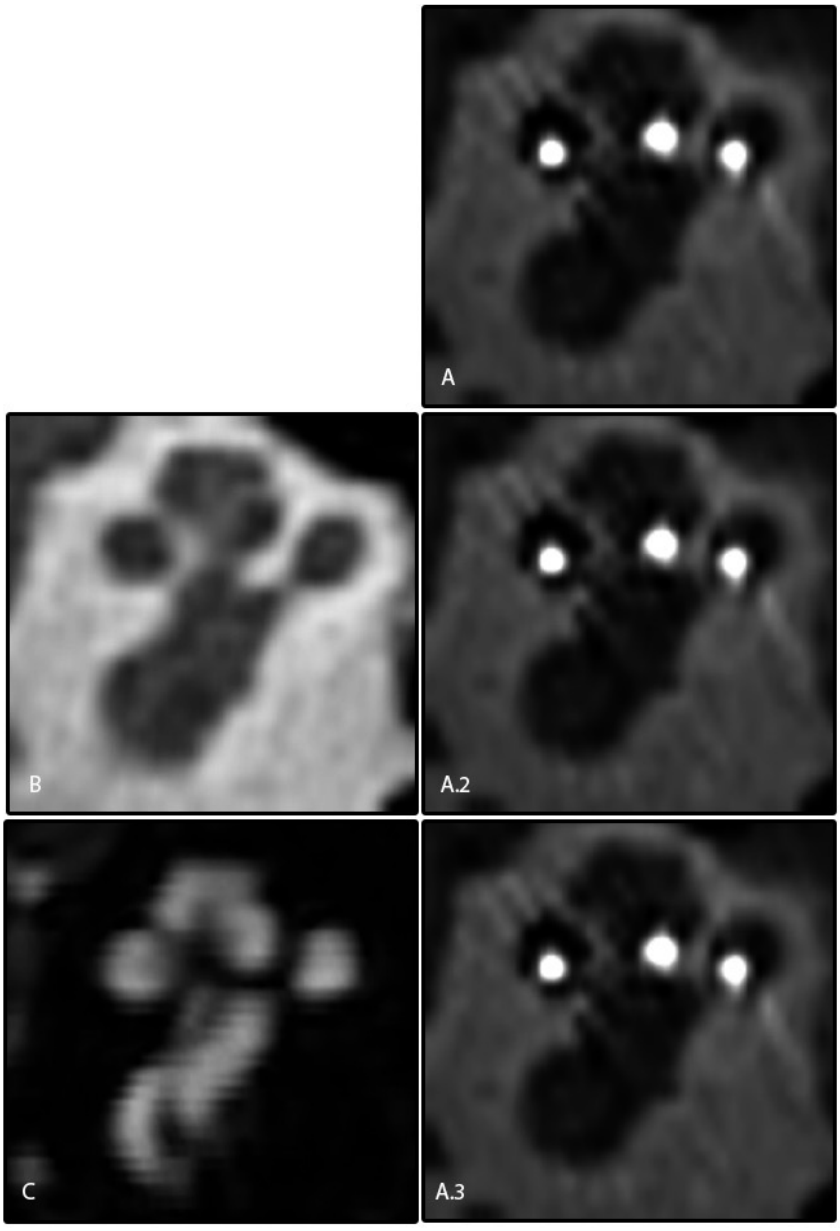

Figure 1: Midmodiolar cross-sectional postoperative CT-images (A), and spatially synchronized CT (B) and MR (C) images.

Statistical analysis

Statistical analyses were performed with SPSS (version 20; IBM, Armonk, New York). To evaluate demographic differences between patients that received the HiFocus MS and the HiFocus 1J implants, a student's T-test for continuous and a chi-square test for categorical outcomes was used. Student's T test was also used to determine differences between groups for the angular insertion depth (Table 1).

Table 1. Demographic characteristics of the studied population

	HiFocus 1J	HiFocus MS	
Patient characteristics			
Implant design (N)	15	15	NS
Age, years (mean ± SD)	58 ± 14	58±18	NS
Male: female	10:5	6:9	NS
Side (AS:AD)	7:8	5:10	NS
Surgical characteristics			
Angular insertion depth, degrees (mean ± SD)	447 ± 57	424±28	P = 0.039
Surgical approach			
Extended RW insertion	15	11	P < 0.000
RW insertion	0	4	

Abbreviations: MS: pre-curved HiFocus Mid-Scala; 1J: straight HiFocus 1J; AS: left ear; AD: right ear; RW: round window

Scores were evaluated on a continuous scale. This choice is justified by the fact that rater disagreement mostly occurs between adjacent score values for which a comparable scale can be assumed. The intra-class correlation (ICC) was calculated for both inter- and intra-observer agreements using the SPSS Reliability-analysis, with a two-way random-effect model. All samples were rated by all raters two times and intra-observer ICC reflects how consistent each rater repeatedly scored the same sample. The inter-observer ICC reflects how consistent the different raters scored the same sample. The ICC was calculated for each electrode contact separately, using the average of the two ratings per observer. These ICC values were used as outcomes in a linear mixed model to evaluate the effect of evaluation method, observer and angular insertion depth on rater agreement as measured by the ICC. From clinical perspective, we were interested in the effect of adding a referential framework based on pre-operative scans. Therefore, for prior analysis, the ICC outcomes for the methods with pre-operative CT and MR images were analysed as one group and compared with the outcomes based on the post-operative scans alone. All electrodes were included in this analysis and a random effect for electrode was used to reflect the correlation between ICCs of neighboring electrodes. This analysis was stratified per implant design.

Table 2. Distribution of scores

	Without	+ CT	+MRI
Score 5: certain SV	101	222	252
Score 4: likely SV	375	383	261
Score 3: intermediate	608	659	546
Score 2: likely ST	1164	731	658
Score 1: certain ST	626	879	1161
Score 0: not assessable	6	6	2
Total of scores	2880	2880	2880

Results

Table 1 demonstrates the comparison of the 1J and MS population. As expected based on the different designs, a significant difference in angular insertion depth exists between the two groups, with the 1J electrode array being on average 33 angular degrees more deeply inserted. Additionally, the average insertion depth of the HiFocus 1J population is on average 33 degrees shallower compared to previous reports from our 1J population[6,7]. The HiFocus 1J is not compatible with a pure RW insertion, and all these electrode arrays were inserted through an extended window approach. Four HiFocus MS implants were inserted through a round window approach. All other characteristics did not differ significantly between the two groups. A total of 8640 scores were included in the analyses. Table 2 shows the distribution of all scores, per method of evaluation. The most notable differences between methods were reflected in scores 1 and 2.

Inter- and intra-observer agreement

The inter- and intra-observer ICCs were calculated for each individual electrode contact within the 1J and MS population separately. The average inter- and intra-observer ICCs per electrode contact for each method of evaluation are shown in Figure 2A and 2B, respectively. It is immediately noticeable that the ICCs show different patterns in the 1J and MS population, for both the inter- and intra-observer ICCs. In the MS population the ICC scores increase from basal to apical contact. The consistency of scores within and between observers for the 1J electrode array shows a more irregular pattern with the highest conformity at the basal contacts. Table 3 and 4 present an overview of the mean and standard deviations of the inter- and intra-observer ICC per method and implant design. Differences in inter-observer ICC's, were only significant between group 1 (only postop images) and group 3 (adding MR) in the 1J ($p = 0.048$) and MS ($p = 0.047$) population. For the mean intra-observer ICC in the 1J population, the ICC's are significantly different between using no pre-operative images and adding CT (1J: $p = 0.008$, MS: $p = 0.002$) or MRI (1J: $p = 0.044$, MS: $p = 0.026$).

Table 3. Inter-observer ICC

	Without	+ CT	+MRI
HiFocus MS (mean, SD)	0,767 (0.234)	0,830 (0.140)	0,829 (0.157)
HiFocus 1J (mean, SD)	0,727 (0.129)	0,781 (0.092)	0,785 (0.081)

A linear mixed model analysis for the inter-observer ICC in the 1J population showed a significant effect for method (p = 0.015), with a 0,047 lower ICC when no pre-operative support was used. We found no significant effect of angular insertion depth on the inter-observer ICC. In the MS population, the inter-observer ICC was 0,062 lower when no pre-operative support was used (p = 0.025). There was an effect of angular insertion depth on the inter-observer ICC found, with an increase of 0,012 ICC per angular degree.

For evaluation of the intra-observer ICC, also the variable 'observer' was included in the linear mixed model. This revealed a significant effect of method (p < 0.001) and observer (p = 0.015) for the 1J electrode arrays. Using no referential framework resulted in 0.091 lower ICC's. Observer 3 scored a 0.0844 lower ICC compared to observer 1 (p = 0.004). No significant difference was found between observer pairs 3/2 and 1/2. In addition, no significant effect of angular insertion depth was found. For the MS implant design, a significant effect of method (p < 0.001), angular insertion depth (p < 0.001) and observer (p = 0.008) was found. Using no pre-operative support resulted in a 0,107 lower ICC. On average, a one angular degree deeper located electrode contact showed a 0,001 higher intra-observer ICC. Additionally, the model showed a 0,061 lower ICC for observer 3 compared to observer 1 (p = 0.002), and a 0,091 lower ICC compared to observer 2 (p = 0.039).

Table 4. Intra-observer ICC

HiFocus MS	**Without**	**+ CT**	**+MRI**
Observer 1 (mean, SD)	0,771 (0.214)	0,942 (0.059)	0,853 (0.260)
Observer 2 (mean, SD)	0,746 (0.249)	0,849 (0.162)	0,883 (0.181)
Observer 3 (mean, SD)	0,714 (0.265)	0,794 (0.129)	0,784 (0.221)
Average 3 observers (mean, SD)	0.744 (0.226)	0.861 (0.095)	0.840 (0.179)
HiFocus 1J	**Without**	**+ CT**	**+MRI**
Observer 1 (mean, SD)	0,764 (0.213)	0,854 (0.076)	0,853 (0.118)
Observer 2 (mean, SD)	0,717 (0.100)	0,802 (0.084)	0,845 (0.086)
Observer 3 (mean, SD)	0,687 (0.216)	0,774 (0.179)	0,756 (0.186)
Average 3 observers (mean, SD)	0.723 (0.122)	0.810 (0.081)	0.818 (0.091)

Abbreviations:

MS = mid-scalar, CI = cochlear implant, ST = scala tympani, SV = scala vestibuli,

ICC = intra- or interclass correlation coefficient, MPR = multiplanar reconstruction

Likelihood of allocated intra-scalar positions

To reflect the certainty of assessments, the percentage of certain versus likely allocations of ST and SV positions were compared. For the 1J electrode arrays, the percentage of certain ST allocations rose from 22.4% to 44.0%, when referential CT images, and to 56.0%, when referential MRI images were employed ($p<0.001$). The percentage of certain SV allocations improved from 16.9% to 23.1%, when CT images, and to 35.3%, when MRI images were employed ($p = 0.007$). Within the MS population, the percentage of certain ST allocations increased from 44.2% to 61.2% and 70.0% with the use of referential CT and MR images, respectively ($p = 0.016$). The percentage of certain SV allocations changed from 24.5% to 50.8% and 59.0% with the use of pre-operative CT and MRI respectively ($p = 0.05$).

Discussion

In this study, we evaluated an easily applicable and reproducible method for determining the intra-scalar position of electrode arrays after cochlear implantation. This method uses spatially synchronized, pre- and post-operative midmodiolar cross-sectional images, presented adjacently, for identifying the scalar boundaries to support localization of cochlear implant electrode arrays. The addition of pre-operative CT or MR images used as reference for the post-operative images significantly improved the consistency of evaluations, demonstrated by increased inter- and intra-observer agreements. This method also increased the certainty of the observers in assessing implant positions. Subsequently, we found no additional, significant benefit of pre-operative MR images in comparison with pre-operative CT images, despite the increased intra- and inter ICC's in the 1J population, when MR images were added. Additionally, our data shows that the consistency and assuredness is highly dependent on angular insertion depth, implant design and its related intra-scalar position. The latter was evidently reflected by the difference in ICC's between the basal and apical contacts in the HiFocus MS population, which differ both in distance between electrode contact and modiolus and in intra-scalar position in superior-inferior direction. Additionally, level of experience also determines the reliability of the evaluation of the intra-scalar position of the electrode contact.

In our study, we demonstrated that angular insertion depth of an electrode contact has a significant effect on both intra- and inter-observer correlations, but only in the MS population. Against expectations, an increase in reliability was found for more deeply inserted electrode arrays and for the more apical contacts. The opposite was assumed because of the decreased size of the anatomical structures in the apical region, which makes it more difficult to distinguish the scalar boundaries. However, this finding might be explained by the in general shallower angular insertion depth of this implant design compared to the 1J electrode array, resulting in less difference between the size of the cochlear lumen at the

tip and the most basal electrode contact of the array. Additionally, we observed that the HiFocus MS electrode array is frequently positioned at the bottom of the scala tympani at the apical region because of the increase vertical stiffness, making it easier to determine its scalar location. This underlines the consequence of electrode design on the evaluation of the intra-scalar localization.

Midmodiolar cross-sectional images are commonly used to evaluate cochlear implant positions, in both ex- and in-vivo studies, and with different modalities.[2,8–10] The latest generation CT scanners have achieved improvements in image resolution, facilitating the use of midmodiolar reconstructions of clinical CT scans as a valuable radiologic tool for predicting electrode array positions. In a clinical study from Lane et al.[11] multiplanar reconstructions of CT scans were used to localize cochlear implant electrode arrays, after validating this particular method with micro-CT.[12] They evaluated 23 electrode arrays on multiplanar reconstructions derived from CT images. With this method, they assessed the positions of 16 (70%) of the electrode arrays within the basal turn. The other 7 (30%) electrode arrays could not be localized, due to pathology that obscured the depiction of the scalar boundaries; i.e., retrofenestral otosclerosis, labyrinthitis ossificans, and incomplete partitioning. In our study, patients with pathological findings on pre-operative images were excluded from participation and 99,84% of the electrode contacts could be localized. Furthermore, in their study they only evaluated the electrode contacts within the basal cochlear turn, because localization of the electrode array beyond the basal turn was considered less reliable, due to the limited depiction of the spiral lamina more apical and the decreasing calibre of the cochlear lumen. In our study, we performed evaluations along the entire length of the electrode array, in order to assess translocations beyond 360 angular degrees.

Other scan modalities have been proposed as clinical tools for implant position evaluations. In a study by Aschendorff et al.[8], rotational tomography offered superior quality over spiral CT. Compared to single- and multirow detector CT, the resolution of rotational tomography was superior, because it provided a more precise definition of the electrode and less metal artefacts. Nevertheless, this technique was rarely described in scientific studies after 2005. Fischer et al.[13] used conebeam computed tomography (CBCT) to determine the scalar position of electrodes. The main advantages of the CBCT over the conventional CT are its lower sensitivity to metal disturbances and its high resolution. Although these two scan modalities were not included in our study, the method used here is also applicable to these scan modalities.

Skinner et al.[10] and Finley et al.[14] used rigid registration of clinical CTs and a high resolution atlas, based on micro-CT and orthogonal-plane fluorescence sectioning microscopy images, to determine in vivo electrode positions. However, from earlier studies, we have learned

that cochlear morphology is highly variable.[6,15,16] This variability implies that the use of a single male donor would not suffice for all implanted patients, unless the atlas could be tailored to match patient-specific morphological characteristics by stretching, tilting, or rotating, as used in rigid registration techniques described by Cakir et al[17]. This limitation led to the method of using multiple atlases,[18] and eventually, using the patient's own pre-operative CT scans as a reference for the anatomical structures of interest.[19] In some institutions, pre-operative images are not acquired in the standard work-up of candidates for cochlear implants. In those cases, the morphological appearance of the contralateral inner ear on the post-operative scan can be used for alignment, because in most cases the ears are highly symmetric for the purposes of cochlear implants.[20] It is difficult to compare the previous methods with our method, in terms of accuracy. However, a primary advantage of our method was that it required no additional appliances, other than those used for routine clinical actions, in contrast to the above described registration methods.

Previous studies have not described the use of MRIs for evaluating the intra-scalar position of the CI electrode. Post-implantation, MRI use is restricted, due to the risk that the electrode array might shift or heat up due to the magnetic field of. Although the magnet of some implants are designed to withstand MRI examinations at 1.5 or even 3 Tesla, clinicians are reluctant to use MRI, because they obviously wish to avoid such adverse events. In our institution, both MRI and CT images are acquired as part of the standard pre-operative work-up for CI candidates. MRI allows the detection of nerve anomalies and can depict obliteration or incomplete partitioning of the cochlea. Midmodiolar cross-sectional MRIs show specific structures of interest, like the osseous spiral lamina and the interscalar septum, in higher detail compared to CT images. A recent study demonstrated that the 7 Tesla MRI provided further improved visualization of certain anatomical details of the inner ear, compared to 3 Tesla images.[21] In the present study, however, we found no difference or additional value between CTs and MRIs in terms of consistency in scoring. This might be the result of image quality degradation following creating MPR's or otherwise because of the already high quality of the CT images. However, the use of 7 Tesla MRI could potentially offer more benefit, when implemented with our method for determining the intra-scalar position of electrode arrays.

Conclusion

This study evaluated the use of spatially synchronized multiplanar reconstructions based on CT and MR images acquired pre- and post-implantation. We demonstrated that this method was an easily applicable approach for determining the intra-scalar position of an electrode array, is more reliable than the use of postoperative images alone and provides

the observers more certainty in their assessment. This method can be used to examine insertion traumas in a clinical setting.

References

1. Hoskison E, Mitchell S, Coulson C. Systematic review: Radiological and histological evidence of cochlear implant insertion trauma in adult patients. *Cochlear Implants Int*. 2017;18(4):192-197. doi:10.1080/14670100.2017.1330735
2. Lecerf P, Bakhos D, Cottier J-P, Lescanne E, Trijolet JP, Robier A. Midmodiolar reconstruction as a valuable tool to determine the exact position of the cochlear implant electrode array. *Otol Neurotol*. 2011;32(7):1075-1081. doi:10.1097/MAO.0b013e318229d4dd
3. Helbig S, Mack M, Schell B, Bratzke H, Stöver T, Helbig M. Scalar localization by computed tomography of cochlear implant electrode carriers designed for deep insertion. *Otol Neurotol*. 2012;33(5):745-750. doi:10.1097/MAO.0b013e318259520c
4. Connor SEJ, Holland NJ, Agger A, et al. Round window electrode insertion potentiates retention in the scala tympani. *Acta Otolaryngol*. 2012;132(9):932-937. doi:10.3109/00016489.2012.680493
5. Verbist BM, Finley CC, Roland PS, Thomas J. Consensus panel on a cochlear coordinate system applicable in histological, physiological and radiological studies of the human cochlea. *Otol neurotol*. 2010;31:722-730.
6. van der Marel KS, Briaire JJ, Wolterbeek R, Snel-Bongers J, Verbist BM, Frijns JHM. Diversity in Cochlear Morphology and Its Influence on Cochlear Implant Electrode Position. *Ear Hear*. November 2013:1-12. doi:10.1097/01.aud.0000436256.06395.63
7. van der Jagt MA, Briaire JJ, Verbist BM, Frijns JHM. Comparison of the HiFocus Mid-Scala and HiFocus 1J Electrode Array: Angular Insertion Depths and Speech Perception Outcomes. *Audiol Neurotol*. 2016:316-325. doi:10.1159/000448581
8. Aschendorff A, Kubalek R, Turowski B, et al. Quality control after cochlear implant surgery by means of rotational tomography. *Otol Neurotol*. 2005;26(1):34-37. http://www.ncbi.nlm.nih.gov/pubmed/15699717.
9. Teymouri J, Hullar TE, Holden TA, Chole RA. Verification of Computed Tomographic Estimates of Cochlear Implant Array Position: A Micro-CT and Histological Analysis. *Otol Neurotol*. 2011;32(6):980-986. doi:10.1097/MAO.0b013e3182255915.Verification
10. Skinner MW, Holden T a., Whiting BR, et al. In Vivo Estimates of the Position of Advanced Bionics Electrode Arrays in the Human Cochlea. *Ann Otol Rhinol Laryngol*. 2007;116(4):2-24. doi:10.1177/000348940711600401
11. Lane JI, Witte RJ, Driscoll CLW, Shallop JK, Beatty CW, Primak AN. Scalar localization of the electrode array after cochlear implantation: clinical experience using 64-slice multidetector computed tomography. *Otol Neurotol*. 2007;28(5):658-662. doi:10.1097/MAO.0b013e3180686e26
12. Lane JI, Driscoll CLW, Witte RJ, Primak A, Lindell EP. Scalar localization of the electrode array after cochlear implantation: a cadaveric validation study comparing 64-slice multidetector computed tomography with microcomputed tomography. *Otol Neurotol*. 2007;28(2):191-194. doi:10.1097/01.mao.0000247817.31572.ed

13. Fischer N, Pinggera L, Weichbold V, Dejaco D, Schmutzhard J, Widmann G. Radiologic and Functional Evaluation of Electrode Dislocation from the Scala Tympani to the Scala Vestibuli in Patients with Cochlear Implants. *Am J neuroradiolgy*. 2015:1-6.
14. Finley CC, Skinner MW. Role of electrode placement as a contributor to variability in cochlear implant outcomes. *Otol Neurotol*. 2008;29(7):920-928.
15. Erixon E, Högstorp H, Wadin K, Rask-Andersen H. Variational anatomy of the human cochlea: implications for cochlear implantation. *Otol Neurotol*. 2009;30(1):14-22. doi:10.1097/MAO.0b013e31818a08e8
16. Jagt AMAV Der, Kalkman RK, Briaire JJ, Verbist BM, Frijns JHM. Variations in cochlear duct shape revealed on clinical CT images with an automatic tracing method. *Sci Rep*. 2017;7(1):1-9. doi:10.1038/s41598-017-16126-6
17. Cakir ÃA, Labadie RF, Zuniga MG, Dawant ÃBM, Noble ÃJH. Evaluation of Rigid Cochlear Models for Measuring Cochlear Implant Electrode Position. 2016:1560-1564. doi:10.1097/MAO.0000000000001245
18. Wanna GB, Noble JH, McRackan TR, et al. Assessment of electrode placement and audiological outcomes in bilateral cochlear implantation. *Otol Neurotol*. 2011;32(3):428-432. doi:10.1097/MAO.0b013e3182096dc2
19. Schuman T a, Noble JH, Wright CG, Wanna GB, Dawant B, Labadie RF. Anatomic verification of a novel method for precise intrascalar localization of cochlear implant electrodes in adult temporal bones using clinically available computed tomography. *Laryngoscope*. 2010;120(11):2277-2283. doi:10.1002/lary.21104
20. Reda F a, McRackan TR, Labadie RF, Dawant BM, Noble JH. Automatic segmentation of intra-cochlear anatomy in post-implantation CT of unilateral cochlear implant recipients. *Med Image Anal*. 2014;18(3):605-615. doi:10.1016/j.media.2014.02.001
21. van der Jagt M a, Brink WM, Versluis MJ, et al. Visualization of Human Inner Ear Anatomy with High-Resolution MR Imaging at 7T: Initial Clinical Assessment. *AJNR Am J Neuroradiol*. August 2014:1-6. doi:10.3174/ajnr.A4084